White Paper #11 – Wind stress and air sea fluxes observations: status, implementation and gaps

Cronin, M.F.[1], Bourassa, M.[2], Clayson, C.A.[3], Edson, J.[4], Fairall, C.[5], Feely, D.[1], Harrison, D.E.[1], Josey, S.[6], Kubota, M.[7], Kumar, B.P.[8], Kutsuwada, K.[7], Large, B.[9], Mathis, J.[1], McPhaden, M.[1], O'Neill, L.[10], Pinker, R.[11], Takahashi, K.[12], Tomita, H.[13], Mathis, J.[8], Weller, R.A.[3], Yu, L.[3], and Zhang, C.[2]

[1] NOAA Pacific Marine Environmental Laboratory, United States
[2] University of Miami, United States
[3] Woods Hole Oceanographic Institute, United States
[4] University of Connecticut, United States
[5] Michigan State University, United States
[6] National Environment Research Council, United Kingdom
[7] Tokai University, Japan
[8] Indian National Center for Ocean Information Services, India
[9] National Center for Atmospheric Research, United States
[10] Oregon State University, United States
[11] University of Maryland, United States
[12] Instituto Geofisico del Peru, Peru
[13] Japan Agency for Marine and Earth Science Technology, Japan

1. Introduction

1.1 Coupling between the Ocean and the Atmosphere in the Tropical Pacific

Coupling between the ocean and the atmosphere in the Tropical Pacific takes place on a broad range of timescales, in different dynamical regimes, and through different mechanisms. On the basin scale, according to the "Bjerknes Feedback", easterly Trade winds, blowing along the equator, result in a thermocline that is deep in the west and shallow in the east. Poleward Ekman divergence and upwelling, associated with the easterly winds, acting on the sloped thermocline then causes the sea surface temperature (SST) to be cooler in the east than in the west. The resulting zonal gradient in surface pressure, in equilibrium with the SST gradient, strengthens the zonal winds, which through upwelling, feedback to the SST zonal gradient, maintaining the "normal" or La Niña conditions. During El Niño, the feedback leads to weaker Trade winds, shallower thermocline in the west, and reduced SST zonal gradient. While the basic coupling mechanism is simple, the mechanisms that lead to the shifts in the feedback are not. Questions remain regarding interactions between the wind-forced thermocline variability and ocean mixed layer, and the effect of the resultant SST variations on the overlying atmosphere. The simplicity of these concepts also belies the range of El Niño Southern Oscillation (ENSO) events that have been observed in recent decades. For example, while the canonical El Niño has largest anomalous warming in the eastern equatorial Pacific, recent events referred to as "Midoki El Niño" have had anomalous warming in the central equatorial Pacific (Ashok et al. 2007, Takahashi et al. 2011). ENSO events have been more frequent in recent years and there is some evidence that extreme El Niño events may become more frequent in a warming world (Cai et al. 2014).

Atmospheric circulation in the tropics and teleconnections between the tropics and extratropics depend fundamentally upon the distribution of atmospheric deep convection (Gill, 1980; Wallace and Gutzler, 1981; Trenberth et al. 1998). It is thus important to understand how convection is organized and how it both affects and is affected by the underlying SST. Due to the nonlinear dependence of saturated specific humidity on temperature (i.e., the Clausius-Clapeyron effect), latent heat loss is amplified over warm water and enhanced latent heating can help destabilize the atmosphere and drive deep convection. Maximum SST creates a low surface pressure center and drives wind convergence. Deep convection thus tends to form over warm water, such as in the western Pacific warm pool, along the thermal equator in the Northern Hemisphere Intertropical Convergence Zone (ITCZ), and in the South Pacific Convergence Zone (SPCZ). Meanwhile, cloudiness associated with convection shades the ocean from solar radiation and convective gustiness enhances the latent and sensible heat fluxes, both of which lead to surface cooling. The intermittency of atmospheric convection helps maintain the warm sea surface in these mean convective regions.

On shorter (meso- to synoptic) timescales, fluctuations in surface wind stress, temperature, and humidity associated with atmospheric deep convective systems induces strong perturbations in air-sea fluxes, which, together with SST, determine how fast the atmospheric boundary layer would recover from being stabilized by convective cold pools and be ready for the next convective event. Erroneous representation of this recovery time in weather and climate models would inevitably introduce biases in their reproduction of precipitation and clouds over the western Pacific warm pool. The diurnal cycle in equatorial surface winds (e.g., Deser and Smith, 1998; Ueyama and Deser, 2008) appears to be driven by direct solar heating of the atmospheric water vapor and to be part of a deep tropospheric overturning cell (Takahashi, 2012), although the connection to the diurnal cycle in deep convection is unclear (Gray and Jacobson, 1977; Randall et al., 1991; Takahashi, 2012). Furthermore, a semi-diurnal cycle can also play a large role in the variability of cloud cover and precipitation. Simulations and forecast of the Madden-Julian Oscillation (MJO) can be improved when SST feedback to the atmosphere is correctly reproduced in models (Seo et al., 2009). The oceanic diurnal cycle plays a special role in air-sea interaction of the warm pool. In regions with low winds such as the western Pacific warm pool, daytime solar warming can lead stratification within the upper 5 meters of the water column (i.e., a "diurnal mixed layer"), so that the SST at 1 m can be significantly cooler than that at the air-sea interface. A shallow diurnal mixed layer can also trap wind-generated momentum, causing large vertical shears in the horizontal velocity. In the early evening, as the stratification weakens, shear instability can then form, causing enhanced turbulent mixing within the upper ocean. There are mixing parameterizations that account for this additional source of turbulence in global Ocean General Circulation Models (OGCMs) (Danabasoglu et al., 2006), but at best, verification has been sparse and indirect.

In the central equatorial Pacific, east of the warm pool boundary, atmospheric convection is normally absent except during the warm phase of the El Niño Southern Oscillation (ENSO) cycle and eastward penetration of extraordinarily strong MJO events.

While equatorial zonal wind stress near the equator, through its effects on upwelling and mixing and on latent and sensible heat loss, plays an essential role in both interannual and intraseasonal variations, surface radiation has been shown to be another necessary ingredient in determining SST in the ENSO cycle. The feedback of SST to the atmosphere is critical in this region to determine the fate of an ENSO or MJO event. Sharp meridional SST gradient exist in the central and eastern equatorial Pacific, between the "equatorial cold tongue" and the warm water beneath the ITCZ, the "thermal equator", which extends across the entire northern tropical Pacific. In contrast, the SPCZ is found mainly in the western tropical Pacific. Coupled models often have an equatorial cold tongue that is too cold and a spurious double ITCZ. Both convergence zones are marked by active synoptic-scale atmospheric perturbations. SST modulation on the SPCZ is a crucial factor in models' ability to reproduce realistic SPCZ or create spurious double ITCZ there.

In the eastern Pacific, atmospheric deep convection is normally confined to the ITCZ north of the equator, except during the peak phase of an ENSO warm event. In the SST front, between the equatorial cold tongue and the warm water of the thermal equator, tropical instability waves (TIW) thrive. The air-sea coupling associated with TIW take place through both modulation of the atmospheric boundary-layer (ABL) stability and barometric pressure gradients induced by the SST front (Chelton et al., 2001; Cronin et al. 2003): the barometric pressure effect results in stronger winds at the SST front; the destabilization of the ABL leads to vigorous vertical mixing that brings larger winds from aloft to the surface on the warm side of the front. This acceleration of the surface wind across the equatorial cold tongue SST front and convergence over the warm "thermal equator" is pivotal in determining the location of the ITCZ and double ITCZ (in boreal spring). Available evidence, however, is conflicting on whether the ascent in the ITCZ in the eastern Pacific is shallow (Zhang et al., 2004; Back and Bretherton, 2006) or deep (Schumacher et al., 2004). The ascending motion in the ITCZ helps form the upward branch of the Hadley cell in boreal summer, with its associated descending branches over the subtropical North and South Pacific. These descending motions are the essential ingredients for marine stratus clouds over the northeastern and southeastern Pacific, which are key components in the Earth's radiation budget but poorly simulated in climate models. How these marine stratus clouds may vary in and feedback to a changing climate is a major uncertainty in ENSO simulations and climate projections. The air-sea coupling processes that determine the position, structure, and strength of the ITCZ must be better understood in order to improve coupled model representations of atmospheric ENSO feedbacks (e.g. Lloyd et al., 2009) and cloud feedback on seasonal-to-interannual and climate change time-scales (Lengaigne and Vecchi, 2010; Cai et al., 2014).

The large-scale mean and interannual convection patterns comprise systems of a variety of scales including mesoscale, diurnal, synoptic, intraseasonal and seasonal. How these different scales interact, and likewise how these coupled feedbacks and multiscale coupled processes will change in a warming world remain open questions. While the

Tropical Pacific Observing System (TPOS) will not capture all of these processes in their full resolution, it must capture aspects of the multiscale coupled interactions that are critical to the evolving ENSO system.

As described in this white paper, information on surface fluxes and on parameters used in the surface flux computations within the atmospheric and oceanic boundary layers are needed to initialize, force, and nudge numerical models; to assess uncertainties in these numerical models and in satellite observations; and to better understand the coupled system and improve numerical model representations of this system. As such, it is critical that the observing array have coverage not only in regions where the coupled processes are most active for ENSO (i.e. in the western Pacific and along the equator), but also in regions where biases and large uncertainties exist in satellite data and numerical model output (e.g. along the ITCZ and SPCZ latitudes).

1.2 Estimating fluxes of heat, moisture, momentum, and CO_2

The 2020 Tropical Pacific observing array will be integrated, with observing platforms that measure numerous variables. As described in this section, estimation of any turbulent air-sea flux, whether it be heat, moisture, momentum or gas, requires a common set of variables, including SST, wind, air temperature and humidity. It is therefore important to consider the larger goals and requirements for all air-sea flux observations. Locations of moored buoys, including those with net surface heat flux measuring capabilities, are shown in Figure 1.1.
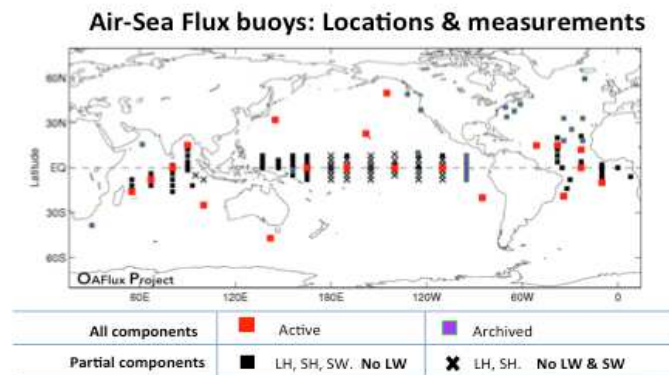

Figure 1.1 – Global distribution of flux and flux parameters.

Calculation of air-sea heat, moisture, momentum and gas exchanges are discussed at length elsewhere (e.g., McGillis et al., 2001; Fairall et al., 2003) and therefore will only be briefly discussed here. In particular, direct estimates of turbulent fluxes (e.g. wind stress, evaporation, latent and sensible heat, and CO_2 fluxes) require high frequency samples of the 3-component wind plus the appropriate scalar parameter, from which the covariance (turbulent flux) can be computed after removal, when necessary, of platform motion (e.g., Ancil et al., 1994; Edson et al., 1998). These measurements must be made within the surface layer directly above the air-sea interface, preferably above the wave-influenced flow but still within the layer where the turbulent fluxes are vertically uniform. By law of the wall arguments, the wind and parameter profiles vary logarithmically with

height within this "constant flux layer". Typically this layer extends from roughly 2 m to 50 m above the interface, with the variability largely a function of wind speed and stratification. Modern bulk algorithms, based upon this physics, estimate turbulent fluxes from two observations of state variables (at least wind, temperature and humidity) from different heights near the surface and within the "constant flux" portion of the atmospheric profile.

These measurements however are not sufficient to directly estimate the fluxes. Several aspects of the profiles must be parameterized and therefore introduce errors in the fluxes. In particular, the atmospheric stability can affect the shape of the profiles and must be parameterized based upon the measured quantities (primarily air-sea temperature difference). The atmospheric stability can also affect the gustiness. The COARE bulk algorithm (Fairall et al., 1996a, 2003, 2011, Edson et al., 2013) computes a gustiness parameter assuming that the wind measurements are hourly vector averages. Cronin et al. (2006b) show that if the vector wind speed is based upon daily averages, such as is the case when using telemetered TAO data from the legacy ATLAS systems, the mean error associated with the scalar wind speed can increase to more than 1.5 m/s, causing an 8 W/m^2 bias in the latent heat flux in the ITCZ regions. Likewise, the roughness layer is generally parameterized in terms of wind speed, although some newer parameterizations also take into consideration surface wave characteristic (e.g. significant wave height and/or dominant wave period). The influence of other wave characteristics, such as steepness, age, breaking, white-capping, direction of propagation relative to the wind and the presence or absence of swell, is much less understood. Other complicating factors for flux calculations include rainfall, surfactants, and the relationship of the interface "skin" temperature to the measured bulk sea surface temperature. Measurements of these parameters under a full range of weather conditions are required to understand these effects on surface fluxes and for improving the flux parameterizations. Given this parameterization complexity, the TPOS should include flux observations from both bulk observations and direct measurements via turbulent covariance packages mounted on surface moorings (e.g., Ancil et al., 1994; Weller et al., 2012; Bigorre et al., 2013) and on research vessels maintaining the TPOS.

Table 1.1 - Observations required for evaluation of air-sea fluxes of momentum (TAU), heat (Q0), and moisture (Evaporation minus Precipitation); accuracy and standard deviation of a daily averaged measurement; and contribution of this error to the error in the air-sea fluxes. The signal-to-noise factor is the accuracy divided by the standard deviation and can be used to determine the sensitivity of the flux measurement to the flux parameter. The total measurement errors assume that these errors are independent and do not include errors associated with the bulk algorithm. Variables listed in bold font are flux variables; others are flux parameters.

		For daily averages			Contribution to		
	Flux	**er**	**Std**	**Std/er**	**er(TAU)**	**er(Q0)**	**er(E-P)**
Variable					Nt/m^2	W/m^2	mm/day
wind speed (m/s)	all	0.1	1.75	17.5	0.0027	2.1	0.053
SST (C)	all	0.1	1.45	14.5	0.0002	4.4	0.081

Variable					TAU	Q0	E, P, E-P
air temp. (C)	all	0.1	1.30	13.0	0.0002	3.6	0.075
rel. hum. (percent)	all	2.7	4.83	1.8	0.0002	11.9	0.32
SWR (W/m^2)	Q0	6	42.00	7.0	0	5.6	0
LWR (W/m^2)	Q0	4	13.75	3.4	0	3	0
sfc currents (m/s)	all	0.05	0.25	5.0	0.0008	0.65	0.017
BP (hPa)	FCO2	0.2	1.48	7.4	0	0	0
Rain (mm/day)	E-P	0.72	5.34	7.4	0	0	0.7
Total of meas. errors					**0.0027**	**14.3**	**0.81**
Meas. error for covariance fluxes					0.0008	8.2	0.7
Total meas. and sampling error for cov. fluxes					**0.0021**	**9.2**	**0.7**
					TAU	**Q0**	**E, P, E-P**
Mean (across equator)					0.039	125.6	2.0,1.9,0.12

Table 1.1 summarizes the accuracy of state variables measured from the Tropical Pacific mooring array as of 2005 (Colbo and Weller, 2009; Freitag et al., 1994), their signal-to-noise ratio, and their contribution to errors in the fluxes. These flux errors assume mean values averaged across the full equatorial Pacific. It should be noted that because of non-linearities (e.g., Clasius-Clapeyron), sensitivities to errors may be larger in the western Pacific than in the eastern Pacific. The standard suite of moored surface measurements (i.e., wind speed and direction, air temperature, relative humidity, and SST) are the most important state variables, being required for estimating all turbulent air-sea fluxes. In contrast, air-sea fluxes are relatively insensitive to barometric pressure variability and can be represented by its mean value. Likewise, because net longwave radiation has relatively small temporal variability in the tropics (Pinker et al., 2013), it is often parameterized in terms of other state variables (Fung et al., 1984; Gupta et al., 1992; Wang et al., 2000). These parameterizations however have an RMS error of ~12 W/m^2 (Cronin et al., 2006b) and thus will increase the error in the net surface heat flux above the target 10 W/m^2. It should also be noted that these variables can serve other purposes beside their role as state variables in flux calculations: Because of the geostrophic relationship between winds and pressure, barometric pressure, when assimilated into atmospheric models, can help produce more accurate representation of synoptic weather fields. Downwelling longwave radiation, in comparison to solar radiation and their clearsky values can provide important information about cloud properties. Directly measured downwelling longwave radiation are also important to evaluate various indirect techniques of estimating downwelling longwave radiation considering that none of those techniques have emerged as appropriate for different climate condition.

As shown in Table 1.1, due to the poor relative humidity sensor accuracy (Freitag et al., 1994), the 2005 TAO suite of sensors does not meet the target benchmark accuracy of ±10 W/m^2 for net surface heat flux when averaged over a day. With a more accurate humidity sensor this target could be met. New sensors are being evaluated for Ocean Climate Station moorings and PMEL RAMA and PIRATA moorings. Likewise, SST (i.e., skin temperature) error contributes substantially to the net surface heat flux errors. Much of this error is associated with the diurnal warm layer and cool skin that cause the bulk SST at 1 m to differ from the skin temperature (Clayson and Bogdanoff, 2013). Present corrections are based upon simple wind speed and/or 1-dimensional models that require full radiation and state variable estimates. With improvements in these models, the SST error might be reduced by as much as an order of magnitude. Rainfall is extremely hard to measure at sea, and its sampling errors are very large on 1-day time scales. The largest systematic error associated with this measurement is low catchment due to wind blowing the rain over the sensor rather than allowing precipitation to fall into the catchment. This however can be corrected to a certain extent (Serra et al., 2001), if wind measurements are collocated with the rain measurement, as is assumed in Table 1.1. With turbulent fluxes measured directly by high-frequency covariance methods, the target flux errors could be met. It should be noted that errors due to the bulk algorithm will contribute ±3.5 W/m^2 for a daily averaged Q_0 measurement and about 0.6 mole/m^2/yr to the CO_2 flux. These are not included in the Table 1.1.

1.3 Observing boundary layer processes

Air-sea fluxes influence the atmosphere and ocean most directly within the mixed layers immediately above and below the air-sea interface. The atmospheric boundary layer (ABL), in turn, is strongly connected to the troposphere through mixing and transport across the inversion layer. At present, routine *in situ* observations of the vertical structure of wind, temperature and humidity are made only on a few island stations, and infrequently from research vessels and research aircraft. From 1995-2002, upper-air soundings were launched from the vessel maintaining the 110W and 95W TAO lines in the eastern tropical Pacific. These data provide important information about the seasonal-interannual variations in the atmosphere (Zhang et al., 2004). These measurements, however, are too infrequent to effectively benefit operational weather forecast models. Island-based measurements using radar or radiometric atmospheric profilers (e.g. Ware et al., 2003), combined with planetary boundary layer soundings using tethered balloons (which could include turbulence measurements, i.e. Balsley et al., 2006) and surface meteorological stations would be an efficient way of providing continuous monitoring that would resolve the diurnal cycle of the lower atmosphere. The viability of using islands (Figure 1.2) as measurement stations was proven by the multiyear TOGA enhanced atmospheric network in the equatorial Pacific (McPhaden et al., 1998). Additionally, with engineering, repackaging, and testing, buoy technology may exist in 2020 that resolves ABL wind profiles and their variations down to the diurnal cycle. These measurements could be extremely useful for initializing operational models, validating climate models, calibrating satellites, observing flux parameters above the surface wave regime, and for studying boundary layer processes, particularly in areas of

thin boundary layers or strong advection. Observing profiles above the roughness layer is of practical importance for small platforms that do not have a tower. Their measurements may be shielded by waves and not capture the open-ocean surface meteorological conditions. It is recommended that atmospheric and oceanic boundary layer observations should routinely be made during the tropical Pacific mooring maintenance cruises. Furthermore, continuous atmospheric boundary layer profile and surface observations should be made at island and/or buoy sites.
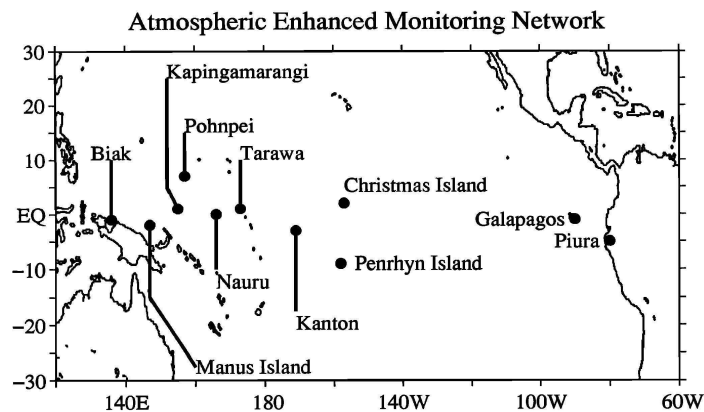
Figure 1.2 – Locations of wind profiler and radiosounding stations during TOGA (from McPhaden et al., 1998).

Within the ocean, temperature and salinity profiles have been measured by sensors attached to the surface mooring lines and by Argo floats. As discussed in the previous section, within the top 2 m, on days with light wind, a diurnal "warm layer" can form that can cause the "bulk" SST to differ substantially from the "skin" temperature felt by the atmosphere. High-resolution (e.g. 10 cm in vertical) Argo floats provide one of the few ways to directly measuring this layer. At nighttime, the homogenous "mixed layer" typically extends to ~20 m. It should be noted that while TRITON moorings and the equatorial TAO moorings resolve the mixed layer, many of the off-equatorial TAO moorings measure subsurface at intervals of 20 m and thus do not resolve the 0-25 m diurnal mixed layer. By their nature Argo floats are not at fixed location and are not co-located with air-sea flux measurements or state variables. Surface moorings in contrast, provide the surface and subsurface measurements at a fixed location with time resolution of order minutes. As discussed in the next section, depending upon the purpose of the measurement, these sampling capabilities can be important. Clearly though, at sites that measure fluxes, the mixed layer depth should be measured with similar temporal resolution. Because the diurnal warm layer depends fundamentally upon the absorption of solar warming within the water, which itself depends upon the biota in the water, the phytoplankton distribution can affect SST variability (Siegel et al., 1995, Murtugudde et al., 2002) and even impact ENSO (Jochum et al., 2010) and the large-scale climate system (Patara et al., 2012). Photosynthetically Active Radiation (PAR) and subsurface optical absorption should thus be measured at one or more biogeochemical flux stations in a region of light wind where there may be feedbacks between the diurnal warm layer and phytoplankton blooms. Pending technology

development, observations of the direct and diffuse radiation components at this station would provide invaluable information for the extinction profile in water, for ocean heat budgets, and for cloud studies. Upward looking acoustic Doppler Current Profilers (ADCP) likewise are unable to observe currents above ~30m and thus miss current variability associated with the diurnal mixed layer. To observe currents within the mixed layer, generally current meters must be attached to the mooring line of a surface mooring. New autonomous buoy technology (e.g. wave gliders) are being developed that may provide platforms for downward looking ADCP that could monitor the near-surface layer of direct wind forcing.

2. Air-sea flux observation requirements for satellite products and numerical models

2.1 Initializing, forcing, and nudging models

There are different modeling requirements for Tropical Pacific observations of air-sea fluxes (ASF) and flux parameters (FP). The major ASF dependencies are *flux type*: Upper Atmosphere, UA, (solar, down-welling longwave and precipitation), Turbulent (wind stress, sensible and latent heat, evaporation) and Ocean (upwelling longwave); *model configuration*: AGCM, OGCM and CGCM; and *simulation mode*: Prognostic; Predictive. For each combination, Table 1.2 indicates the primary purpose of the observations: Verification (V), Forcing (F) or Initialization (I). Model configurations are indicated by common examples; Prognostic AMIP (Atmosphere Model Intercomparison Project), CORE (Coordinated Ocean-ice Reference Experiments) and CMIP (Coupled Model Intercomparison Project) and Predictive NWP (Numerical Weather Prediction) including the (re)analysis. A major challenge of atmosphere models is to generate the UA-ASF from the UA-FP, such as clouds, stability and water vapor. The primary Ocean-FP is SST (both skin from remote sensing and bulk from surface buoy and drifters) and up-welling longwave flux is included here, because of its dependence on SST. Ocean surface current is secondary. Bulk formulae parameterize the turbulent fluxes in terms of the SST, and the Atmospheric Surface Layer (ASL)-FP (wind speed, air temperature and humidity). Additional observational requirements for modeling biogeochemical cycles include air and sea pCO_2 and upper ocean pH and O_2.

Table 1.2 – Primary purpose (verification, forcing, or initialization) for air sea flux (ASF) and flux parameter (FP) observations as functions or flux type (upper atmosphere, surface turbulent, oceanic, and atmospheric surface layer), model configuration and simulation mode (i.e., AGCM, OGCM, CGCM, prognostic or predictive).

	UA-ASF	Turb-ASF	Ocean-FP	UA-FP	ASL-FP
AGCM : AMIP	V	V	F	V	V
NWP/Reanalyses	V	V	F	I	I
OGCM : CORE	F	V	V		F
Ocean Prediction	F	V/F	I		F
CGCM : CMIP	V	V	V	V	V
Climate Prediction	I	I	I	I	I

The most common use of ASF and FP is verification of means and of variability from inter-annual to the seasonal cycle (Bates et al., 2012) and diurnal. Fidelity in solutions can be a consequence of compensating flux and model errors. AGCMs use observed SST as boundary condition, so there are requirements for SST to resolve down to the diurnal cycle and to spatially resolve Tropical Instability Waves.

OGCMs forced by air-sea fluxes have been found to drift far away from the SST used to compute the fluxes, but this method should be explored for ocean prediction where the data assimilation can control the drift. Alternatively, the CORE protocol (Griffies et al., 2009) computes fluxes using prognostic model SST with observed ASL-FP and UA-ASF with diurnal resolution. Tropical Pacific observations of these quantities were essential to reducing known global biases to acceptable levels (Large and Yeager, 2009) and will need to continue in case the biases are non-stationary.

The Group for High Resolution Sea Surface Temperature (GHRSST) Development and Implementation Plan (GDIP) (Donlon et al., 2009, 2010) provide numerous recommendations for a global in situ SST observing system that should be considered in the TPOS (see: https://www.ghrsst.org/files/download.php?m=documents&f=OO-ModernEraSST-v3.0.pdf). We highlight several recommendations here:

- GDIP recommends that the number of moored fiducial ("reference") sites with high quality instrumentation should be increased. Uncertainty estimates need to be delivered with all measurements and the depth of SST measurement reported with all measurements. Calibration stability must be assured and ideally demonstrated for all platforms.
- GDIP strongly recommends that all Argo floats be equipped with a capability to make high vertical resolution measurements of SST in the upper 10 m of the ocean surface and that shallow-water Argo floats be developed and deployed.
- GDIP recommends contemporaneous SST and wind stress in order to understand the context of the SST measurement (e.g. cool skin and thermal stratification), and to help blend the SST measurements from different measurements. Steps should be taken to secure high temporal resolution (ideally at an hourly resolution) wind fields over the global ocean for use in diurnal SST variability modeling.
- GDIP recommends that the SST community of producers and users establish and maintain: a. a programme of *in situ* measurements, both thermometers on buoys, ships and subsurface vehicles and radiometers on ships and platforms that can be used for validating the different products. For the sake of efficiency, it is desirable that this be a fully collaborative programme shared between all the agencies responsible for SST products. There is also a need to specify the requirements for new *in situ* data acquisition systems to support data integration, including wider coverage by shipbased radiometers, diurnally resolving moorings, Argo with additional sensors for near-surface sampling and the OceanSites approach.

Finally, initial conditions are paramount for atmosphere, ocean and coupled model predictions, and the assimilation of an observational data stream is an integral part of any system, regardless of the sophistication (from simple nudging to Ensemble Kalman filters). Fully coupled data assimilation where observations on one side of the air-sea interface influences the other and both sides use the same fluxes is the ultimate goal for climate prediction, so the associated research, development and operations require coincident observations of all the ASF and FP.

2.2 Assessing uncertainties in models

In order to understand where observations are most needed for assessing uncertainties in models, it is useful to review common biases. It should be noted however that without distributed high quality reference data, the presence of a bias may not be known (e.g. Figure 2.1).

Atmospheric reanalysis systems combine observations and models to provide global four-dimensional uniformly gridded datasets that are valuable for studying weather systems and climate variability. However, the quality of the reanalyzed air-sea fluxes is highly sensitive to the uncertainties in model parameterizations and to the temporal inhomogeneity of the observing system. For the reanalyzed surface heat fluxes (latent heat flux, sensible heat flux, longwave and shortwave radiation), major sources of uncertainties are attributable to the representation of near-surface physical processes, the choice of parameterization of subgrid-scale turbulent and convective processes, and the assimilation of observations from different platforms that causes spurious trends (Chen et al., 2008).
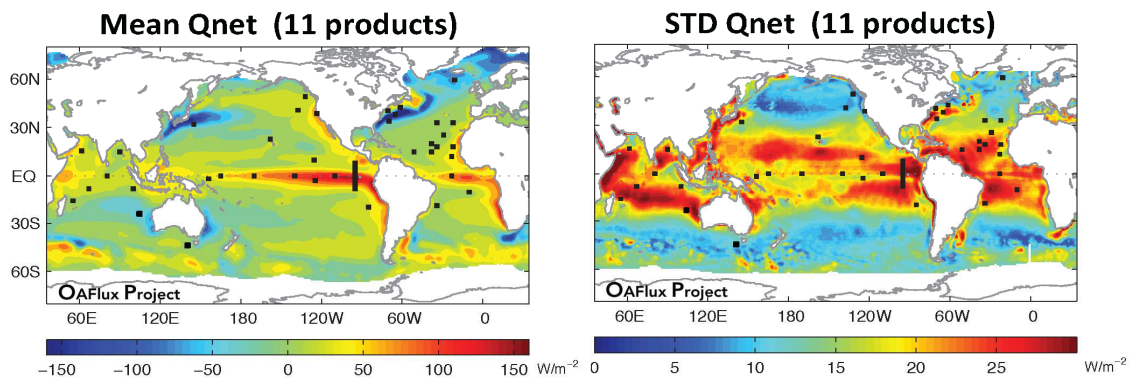

Figure 2.1 - Mean net surface heat flux from 11 products (left) and standard deviation of these 11 products (right). Products include: OAFlux, NOC2, ERAinterim, MERRA, CFSR, ERA40, NCEP1, NCEP2, CORE2, ISCCP, NASA/SRB, CERES. Squares indicate active and historical buoy reference sites.

The downward radiation fluxes at the surface are heavily modified by clouds, and the large uncertainties in the reanalysis cloud parameterizations lead to significant biases in the surface radiative fluxes (Allan et al., 2004). The bias in the incoming solar radiation is the dominant error source in the surface radiation budget over the tropical oceans (Song and Yu, 2013; Cronin et al., 2006b). Reanalyses (ERA40, NCEP/NCAR, and NCEP/DOE) tend to produce too much reflective cloud over the tropical oceans (i.e.,

negative bias in downward solar radiation), except for the stratocumulus regimes where model cloud cover is too low (Betts et al., 2006; Cronin et al., 2006a). The downward longwave radiation at the surface is dependent of the atmospheric structure and composition, as well as cloud base temperature. Differences in the reanalysis longwave radiation in the tropical oceans are also due to the differences in cloud cover and their vertical structure. However, in the tropical regions, which are saturated by water vapor, the water vapor has a strong impact on the downwelling longwave radiation as shown in Nussbaumer and Pinker (2011).

The reanalysis latent and sensible heat fluxes are affected primarily by the biases in near-surface air humidity and temperature (Yu et al., 2008), although the choice of the bulk flux algorithm is also a factor (Smith et al., 2011). Air humidity in all reanalysis products is biased dry in the tropical oceans and hence, contributees to an overestimation of the reanalysis latent heat loss (evaporation) at the ocean surface (Jiang et al., 2005). Overall, the largest uncertainties in the reanalysis heat fluxes are due to the shortwave radiation and latent heat flux components, with the largest errors found off the equator (Figure 2.1).

Reanalysis wind stress show analogous large-scale features, however, differences are noted in the strengths of wind speed and wind stress curl and in the representation of small-scale features, such as the variability on frontal and eddy scales (Milliff et al., 2004; Collin et al., 2012). Differences are also observed in synoptic-scale variability of weather systems. Compared to QuikSCAT winds, reanalyses tend to have storms with larger horizontal extent that lack the depiction of the fine spatial details. The spatial resolution has been improved considerably in the latest reanalysis efforts and ERAinterim and CFSR have a more realistic representation of meso- and synoptic scale wind variability (Jin and Yu, 2013).

Over the tropical oceans, the precipitation in the reanalyses is much greater compared to satellite estimates from GPCP (Bosilovich et al., 2008). The bias in precipitation is consistent with the bias in evaporation. Reanalyses tend to produce excessive evaporation (latent heat loss). Since atmospheric water vapor cannot exceed the saturation limit, the excessive evaporation will lead to an excessive precipitation. Precipitation is an integral component of the water and energy cycles and is also largely related to modeled physical parameterizations. Newman et al. (2000) showed that there is a high internal consistency of precipitation, outgoing longwave radiation, and upper-level divergence within a reanalysis, but a low external consistency (i.e. the agreement between reanalyses), which suggests that the biases in evaporation and precipitation are dependent on the model physics.

While the coupling associated with ENSO is predominately an equatorial zonal process, for understanding the multiscale variability and uncertainties in the global energy balance it is important to monitor the flux parameters and all components of the net surface heat flux in the convective regimes of the western Pacific warm pool, the SPCZ, and ITCZ. Despite the importance of coupled processes in the tropical Pacific and the fact that the Tropical Pacific is larger than the tropical Indian and Atlantic Oceans combined, at present, there are as many active flux stations in the tropical Pacific as in

the tropical Indian Ocean (Figure 1.1); and there are more flux stations in the tropical Atlantic than in either of the other basins. Finally, while both the RAMA and PIRATA arrays have full-flux buoys both on the equator and off, within the tropical Pacific Ocean, all components of the net surface heat flux are presently monitored at only 4 sites along the equatorial Pacific, and at the Stratus mooring (20S, 85W). It is recommended that all components be monitored at several sections that cross the SPCZ and ITCZ. In addition, it is recommended that reference stations be initiated in the Trade wind regime north of the ITCZ, similar to the other basins.

Because models that assimilate observations may not fully manifest the biases included in the physics of the model, it is useful to withhold some observations from assimilation. There are typically two ways this is done: withholding data from the Global Telecommunication System (GTS), or using a WMO number "84" to indicate that these data are reference data and should not be assimilated. We recommend the latter method be used, as these data, whether assimilated or not, can be useful to forecaster analyst interested in validation in real-time. This method however relies upon the operational centers to sort through GTS data and ideally list which data are actually assimilated.

2.3 Common biases in satellite data

Satellite estimates of stress in the tropics are determined from scatterometer observations of equivalent neutral wind (U_{10EN}) relative to the surface current, which is the neutral 10m wind speed required to calculate the friction velocity (squareroot of the kinematic stress) using a neutral drag coefficient (Cardone, 1965; Ross et al., 1985; Cardone et al., 1996; Kara et al., 2008). Spatial oversampling allows estimates on 12.5 to 25 km scales. Scatterometers are wide swath instruments, allowing for calculations of area-averaged spatial derivatives over large areas. These derivatives are noisy unless the averaging scale is three or more times the grid spacing (Holbach and Bourassa, 2013). For rain-free conditions with wind speeds greater than 3 ms^{-1}, the random error in vector components is roughly 0.6 ms^{-1}, with an uncertainty in speed of less than 1 ms^{-1}. There are several additional considerations. For wind speeds <3 ms^{-1} the surface is less homogeneous, making estimation of speed and direction more difficult. Also for these low wind speeds, retrievals tuned to friction velocity have proportionally large bias in stress due to squaring of random errors. And, while strong currents must always be taken into account to obtain an unbiased wind speed analysis from scatterometer observations, in regions such as the Tropical Pacific, where winds are weak and surface currents strong, this is particularly important (Yu and Jin, 2012). Fortunately, because flux models are dependent on the vertical shear in winds, accounting for currents is unnecessary if scatterometer winds are used in the bulk flux models. Rainfall also contributes to larger errors (Draper and Long, 2004; Weissman et al., 2012; and references therein); however, new retrievals that attempt to account for rain (Stiles et al., 2013) are a great improvement over traditional algorithms that were designed only for rain-free conditions. Lastly, the influences of waves on stress should be considered in the neutral drag coefficient used to convert U_{10EN} to stress (Bourassa, 2006; Edson et al., 2013). Most modern flux models are in general agreement regarding the

dependence of the neutral drag coefficient on wind waves. The dependence on remotely forced swell, however, remains highly controversial (Donelan et al., 1997; Bourassa, 2006). The tropical Pacific Ocean has synoptically and seasonally varying swell, which could induce regional and temporally varying biases in surface wind stress.

The most recent release of QuikSCAT winds attempts to adjust for rain related errors, resulting in error characteristics similar to rain-free conditions where such adjustments are possible (Stiles et al., 2013). However, if the rain signal is too strong compared to the wind signal, the scatterometer data are flagged as seriously rain contaminated and generally excluded from further analysis. Not using these flagged data results in much better estimates of stress when compared with collocated data; however, it does bias space- and time-averages of wind stress curl and divergence fields (Milliff et al., 2004). Rain tends to be associated with cyclonic vorticity and convergence, therefore ignoring data associated with rain tends to result in averages and distributions that are biased anticyclonic and divergent.
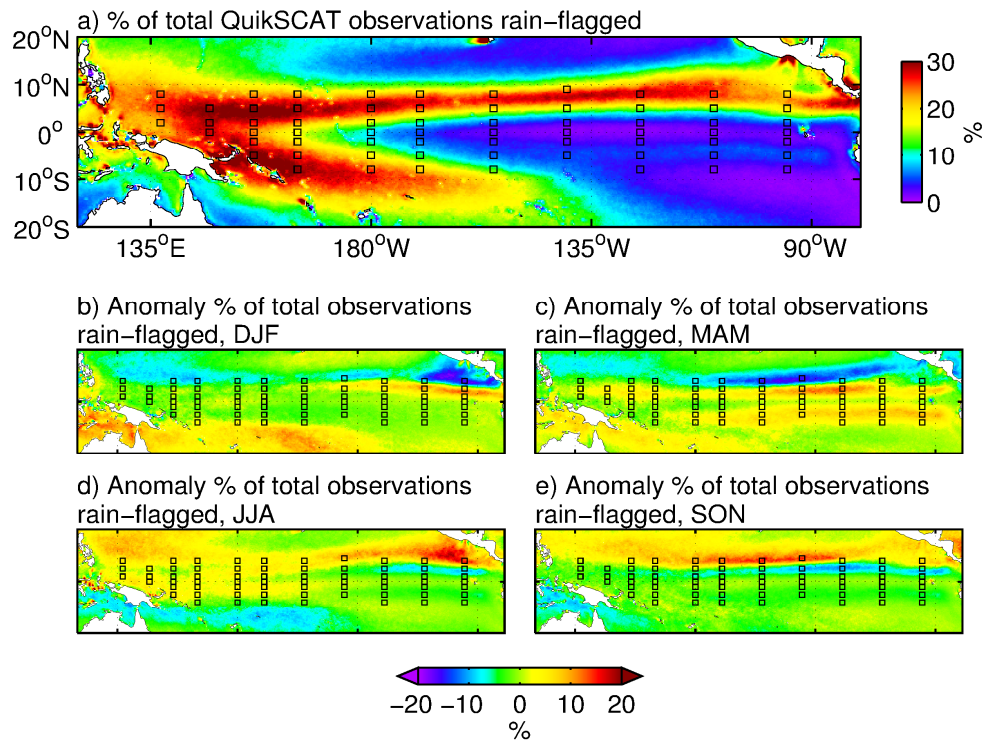

Figure 2.2 – (a) Map of the QuickSCAT rain-flag frequency over the 10-year period August-July 1999; (b-e) seasonal anomalies of the QuickSCAT rain-flag frequency relative to (a). Rain is determined from the QuickSCAT – only rain-flag and a collocted passive radiometer rain rate. The squares in each panel show the locations of the individual buoys in the TAO/TRITON array.

Although intermittent, rain limits the full utilization of QuikSCAT surface winds since rain degrades the ability of Ku-band scatterometers such as QuikSCAT to retrieve accurate vector winds over the ocean. The following examples are based on a product that does not attempt to correct for rain-related errors: they indicate how often rain occurs rather than how often it contributes to serious errors (which is harder to assess). If all

observations flagged as coincident with rain are removed from an analysis, rain-induced sampling biases would be particularly acute in the western tropical Pacific and near the ITCZ and SPCZ, where 20-30% of all scatterometer wind measurements are rain contaminated (Figure 2.2).

During the 10 year period of August–July 2009, rain rarely occurred over the equatorial cold tongue and the southeast equatorial Pacific (<5% of the time). In contrast, the northern and western moorings (squares in Figure 2.2) are well-placed to measure winds in these rainy regions that are not measured accurately by satellite. Such locations will be very important for training wind retrieval algorithms to account for rain, and for determining when such corrections can be usefully done. Figures 2.2b-e show that rain frequency has strong seasonal variability over most of the tropical Pacific moorings.
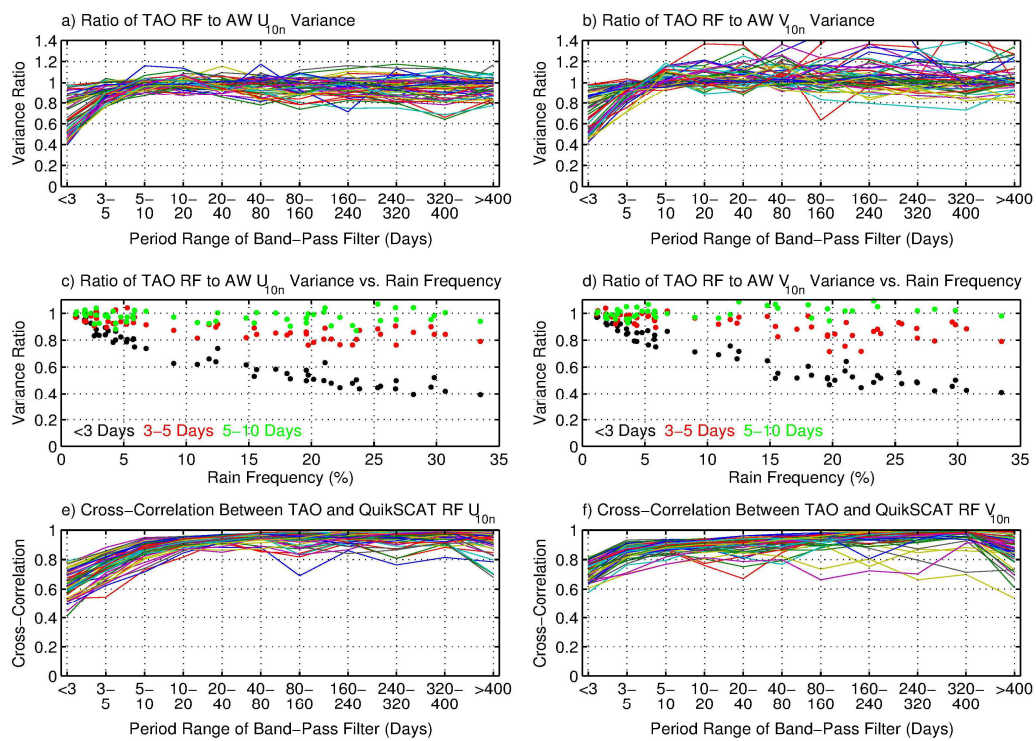
Figure 2.3 - Wind statistics computed over the 10-yr period August 1999-July 2009: (a-b) The ratio of temporal variance between rain-free (RF) and all-weather (AW) TAO equivalent neutral wind (ENW) components as a function of band-pass filtered time period. Each line corresponds to each of the buoys shown in Fig. 4. (c-d) Ratio of TAO rain-free to all-weather wind variances as a function of rain-frequency for each buoy. Black points denote periods less than 3 days, red points are periods of 3-5 days, and green points are periods of 5-10 days. Each point represents an individual buoy. (e-f) Cross-correlation coefficients between the rain-free TAO and QuikSCAT ENW components as a function of band-pass filtered period. Each line corresponds to a different buoy. In all panels, only TAO winds collocated in time and space with QuikSCAT observations were used, and rain occurrence was determined from the QuikSCAT rain-flag. The RSS QuikSCAT dataset was used in these comparisons.

In light of the strong spatial and temporal rain variability, *in situ* TAO wind measurements, that provide all-weather sampling, are particularly valuable in the tropical Pacific. To demonstrate importance of all-weather sampling, TAO winds are used to compute the ratio of variances of rain-free and all-weather time series of zonal U_{10EN} and meridional V_{10EN} wind components at each buoy location shown in Fig. 2.2. Fig. 2.3a, b shows this variance ratio as a function of time-scale. For time-scales less than 5 days, the rain-free time series contain significantly less variance (due to exclusion of rain-flagged data) than the all-weather time-series, while longer than 5 days, the rain-free and all-weather variances are nearly equal. TAO wind measurements provide important information on temporal variability on time-scales less than 5 days that is degraded significantly in rain-free sampling, such as provided by most QuikSCAT products.

As Fig. 5c,d shows, the variance reduction from rain-free sampling is strongly related to rain frequency for periods less than 3 days (black points); frequent rain strongly reduces measured wind variance. For rain frequencies greater than 20%, rain-free sampling captures only about half of the variance of the full all-weather time series. Even relatively modest occurrences of rain, 5% for example, reduces the measured wind variance to only about 80% of the all-weather wind variance. Rain still affects wind variability on time-scales of 3-5 days (red points), although less so; for periods greater than 5 days (green points), the variance ratios approach unity for the whole range of rain frequencies encountered. The effect on time-scales less than 5 days is a consequence of the intermittent nature of precipitating weather disturbance in the tropics. Despite this analysis being based on a worst case assumption of no useful data during rain events, we are confident that qualitatively similar problems exist with the JPL v3 data set for which corrections were attempted.

Cross-correlations between rain-free TAO and QuikSCAT winds are shown in Fig. 2.3e, f. These show that the winds from both platforms are highly correlated for time-scales greater than 5 days. For time-scales less than 3 days, the correlations are all below 0.8. Part of the drop-off in correlation is due to random instrument errors for each platform, but part is due to errors in the satellite rain-flag, which is known to misidentify rain-contaminated grid cells (e.g., Weissman et al., 2012). Thus for assessing uncertainties in satellite scatterometer wind stress, it is recommended to have in situ co-located wind speed and direction, surface currents, SST, air temperature, humidity, and rainfall observations in the convective regions of the western equatorial Pacific, ITCZ and SPCZ. It is also recommended that the future scatterometers (1) have smaller footprints to improve sampling and (2) have a capability of estimating rain rates (e.g., from a radiometer or from using two frequencies for scatterometry).

Estimation of the turbulent fluxes over the oceans from satellites is a still-evolving field. Satellite-derived air-sea fluxes require retrievals of near-surface wind speed, temperature, and humidity, and SST, as well as any additional fields that are needed for the bulk flux parameterization (such as wave information). Issues associated with the wind fields have been noted above, as well as recommendations for improvements to in situ observations of SST. Recent advances have demonstrated improved capabilities of measuring the still-problematic near-surface specific humidity and temperature (Fig. 2.4,

from Roberts et al., 2010; see also Jackson and Wick, 2010; Bourassa et al., 2010; Clayson et al., 2014). Recent estimates of uncertainties of the near-surface temperature and humidity have indicated mean biases of less than 0.1 ^{o}C and 0.2 g kg^{-1}, respectively, are possible. However, there are still regime-based systematic differences between the products and the available observations. Figure 2.5 adapted from Prytherch et al. (2013) shows comparisons of several satellite-based products with the NOC dataset; clear regional biases which appear to be correlated with cloud and weather regimes are evident.
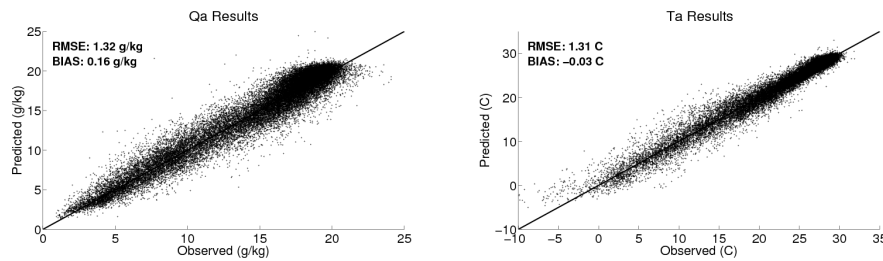
Figure 2.4 - Predicted (satellite-derived) vs. observed parameters for specific humidity (Qa), and air temperature (Ta). The predicted values are the output obtained directly from inversion of satellite brightness temperatures using the neural network as described in Roberts et al. (2010). Observations are from the SeaFlux in situ dataset.
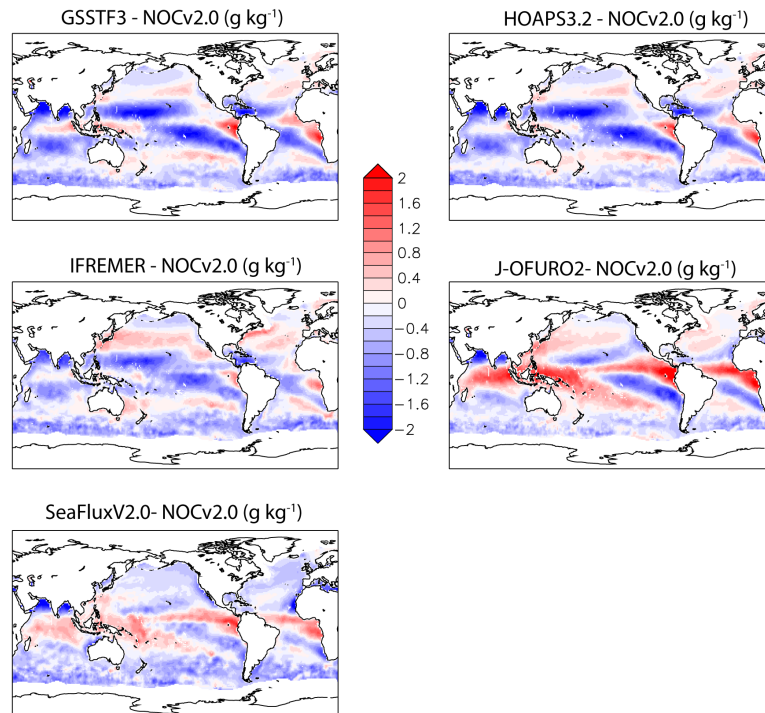

Figure 2.5 - Specific humidity satellite product difference (g kg^{-1}) from observations (satellite product - NOCv2.0, with no uncertainty limit applied), averaged over full period of satellite dataset (from Prytherch et al., 2013).

For the turbulent heat fluxes (and evaporation estimates) it is the difference between the near-surface and surface temperatures and humidities that affect the errors in the retrievals. As reported for one satellite dataset by Clayson et al. (2014), near-stable conditions have much reduced errors than those in highly stable or unstable conditions; extremes in air-sea stratification of humidity likewise have higher errors (Figure 2.6). Given the interest in understanding the distributions of the fluxes and input parameters (e.g. Gulev and Belyaev, 2012), and the importance of understanding the effects of extremes on our weather and climate system, these errors need to be reduced. As shown in Figure 2.7, mean air-sea differences in humidity leading to larger uncertainty are associated with the ITCZ and to a larger extent the SPCZ, while the cold tongue region has the highest mean uncertainty due to stable conditions. Thus to help assess uncertainties in satellite-based retrievals of near surface temperature and humidity, it is recommended that humidity and temperature sensors be collocated with key wind speed and SST measurements in the tropical Pacific.
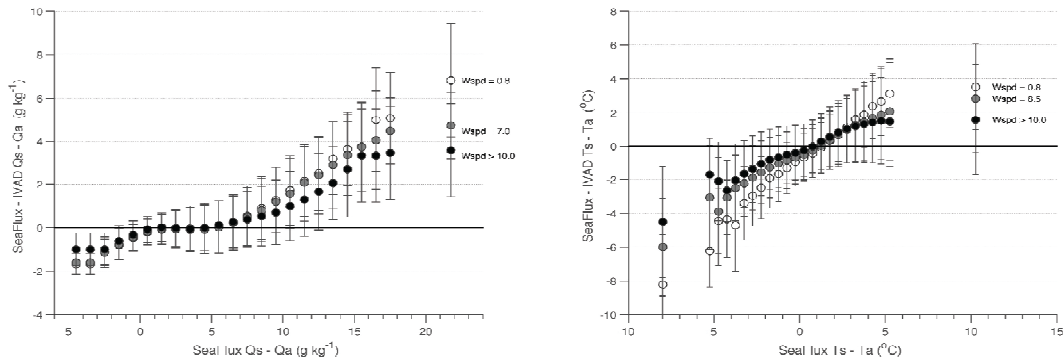

Figure 2.6 - Differences between retrieved satellite values of Qs – Qa and Ts – SST as compared to a matchup-dataset from IVAD, stratified by wind speed (adapted from Clayson et al., 2014).

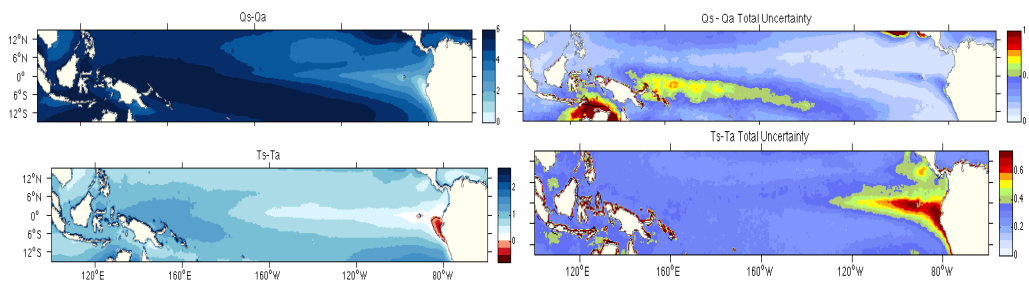Figure 2.7 - Mean air-sea specific humidity difference and uncertainty (g kg^{-1}; top panels) and mean air-surface temperature (^{o}C; bottom panels) from the SeaFlux satellite-based product.

2.4 Air-sea interaction research for improving models

The primary purpose of the TPOS is to monitor developing ENSO conditions. In recent decades there have been dramatic changes in the location, timing, and frequency of the heat anomalies associated with ENSO. Long time series are required to study decadal

variability and long-term changes in ENSO. It is essential that the existing long climate time series of air-sea flux and boundary layer observations continue to be made.

In recent years, there has been a shift in the location of the maximum equatorial heat anomaly associated with El Niño from the eastern Pacific to the central Pacific (Ashok et al., 2007). While some speculate that this is a new type of El Niño, a "Midoki" or pseudo El Niño, others speculate that non-linear dynamics can cause the spatial shift in the anomalies and thus these events are not independent (Takahashi et al., 2011). Clearly, four air-sea flux stations across the entire equatorial Pacific are insufficient to capture these non-linear dynamics. More unsettling however is the fact that these four stations may not have enough zonal resolution to observe the anomaly itself. It is thus recommended that all equatorial sites be enhanced to monitor the air-sea fluxes of heat, moisture and momentum, and the ocean boundary layer temperature, salinity, velocity, and thickness.

As discussed in Section 1.2, estimation of air-sea fluxes from flux parameters, whether observational or numerical, introduces error. Continued research is needed to improve the bulk algorithms used as stand-alone modules, and used within general circulation models. For this purpose, high quality direct observations of the fluxes and the flux parameters used to estimate the fluxes are needed. These have been traditionally made from research vessels and it is recommended that this should be done on the research vessels used to maintain the TPOS. New technology is emerging which allow direct flux estimates to be made from moored buoys as well (Weller et al., 2012; Bigorre et al., 2013). The advantage of the moored measurements is that a wider range of coupled processes are likely to be observed. For example, the surface mooring deployed in the Gulf Stream during the CLIMODE program provided direct measurements of surface stress and buoyancy fluxes over a 15-month period, capturing the full seasonal cycle and atmospheric forcing for 18°C water formation events (Marshall et al., 2009). In addition, the extremely high-resolution geo-positioning information needed for these observations can be used to quantify significant wave height and wave period characteristics. The influence of waves on the wind profile, on flux calculations, on gas exchange, and upper ocean turbulence are all subjects of active research that could be investigated through use of these direct flux sensors (Donelan et al., 1997, Bourassa, 2006; Edson et al., 2013). The disadvantages of these sensors are that they generally require more power, are technologically more complex (and thus more vulnerable to failure), and add expense.

While the covariance flux packages discussed above are used to measure heat and other property fluxes across the air-sea interface, other exciting new technology is making it possible to measure vertical turbulent heat fluxes within the water column. Referred to as Chi-pods, these small sensors can be mounted on the mooring line and deployed for over a year, providing long-term measurements of turbulent mixing (Moum et al., 2013). Mixing is fundamentally how warm surface water is transported downward in the presence of wind-generated Ekman upwelling. Better representation of ocean mixing is needed to improve the coupled ocean-atmosphere models used to forecast ENSO. It is recommended that a subset of the reference mooring sites, both on and off

the equator, be enhanced with Chi-pods and covariance flux packages to provide direct observations of heat fluxes at the air-sea interface and within the water column. The covariance flux packages at the surface should also be used to measure wave height.

Observations that resolve important air-sea interaction processes and mechanism guide and inspire model development and are a cornerstone of efforts to improve numerical models used to forecast ENSO, the biogeochemical response and the ecosystems of the tropical Pacific. As discussed in section 1.1, important open research questions include understanding the role of high-frequency variability and multi-timescale variability: How the diurnal cycle affects MJO, or how MJO affects ENSO, for example, and likewise, how long-term climate change may affect MJO and ENSO. Such multiscale studies require measurements that are both high resolution (order minutes-hours) and long (years-decades). Fixed location data (e.g. mooring data) are ideal for such analyses and it is expected that TPOS mooring array will be the primary data set in many of these studies. To capture the spatial structure in these processes, data from floats, drifters, ships (including the ship servicing the TPOS mooring array) and other platforms within the TPOS must be used. These platforms may not observe all variables with the spatial and temporal resolution needed for the process in question. While not all process studies need to be as large as the TOGA-COARE or EPIC2001 climate experiments, these provide useful framework for how the TPOS ENSO observing array can be enhanced to study climate processes. It is recommended that limited duration, intensive observing arrays be embedded within the TPOS for process studies.

3. Recommendations for 2020 TPOS

For a summary of the air-sea flux and flux parameters deployed in the TPOS of 2005, see Appendix 1. Based upon the discussion within this White Paper, we make the following overall recommendation for the TPOS of 2020:

1. Long climate records should be continued.
2. The research vessel that is used to maintain the observing system should be treated as a platform within the observing system itself, making standard measurements along repeat tracks (e.g. ADCP, CTD, pCO_2, marine meteorology, atmospheric soundings, and other measurements). Emerging technology for making underway CTD measurements that would not impact the required seadays.
3. The TPOS array should integrate multi-disciplinary observations. Data should be freely provided for all users. The array should be designed to provide data needed to observe ENSO events through their full life cycle; to force, initialize, and nudge numerical models; to assess uncertainties in numerical models and satellite products; to calibrate remotely measured variables; to develop and test parameterizations needed for models and satellite products; and to better understand the climate system.
4. Interdisciplinary process studies should be built around the infrastructure of the TPOS.

Specific requirements and recommendations for air-sea flux and wind stress observations within the TPOS 2020 array are as follows. It should be noted that in many cases the present TPOS was designed to meet these requirements.

1. Long climate records from flux stations along the equator should be continued. In addition, wind stress, and all components of the net surface heat and moisture fluxes should be measured at all TPOS longitudes along the equator and at select longitudes off the equator in the convective regions of the western Pacific, SPZC and ITCZ. In the western Pacific, the TRITON buoys could become flux reference stations simply by adding a longwave radiation sensor. Along TAO meridionals such as 140°W, this would require additional shortwave and longwave radiation sensors, and a 10 m current meter. At least one meridional section that crosses the ITCZ should also sample the extratropical trade wind regime north of the ITCZ.

2. All variables, but particularly solar radiation, SST, air temperature, wind, and surface currents need to have their diurnal cycle resolved in near-realtime. Some method for extrapolating bulk SST to skin temperature needs to be used for calculating air-sea fluxes. GDIP recommendations (Donlon et al. 2009, 2010) should be considered for surface temperature observations of the TPOS.

3. All surface buoys should monitor winds, air temperature, relative humidity, and SST as these are state variables for every air-sea flux.   Surface air temperature and humidity estimates from satellites also depend upon many assumptions and parameterizations, and thus have large structural errors that an in situ observing system might resolve. Some off-equatorial "standard" sites may be able to be replaced by small buoy platforms (e.g., mini-TRITON, "easy-to-deploy" buoys, wave gliders,…) that do not have a tower and either are less expensive or require less (or no) ship time. Sensors would be placed on a mast, but must be at least 2 m above the air-sea interface in the mean.

4. The 2020 TPOS array should have a better relative humidity sensor.

5. Atmospheric diurnal-cycle-resolving PBL profiling should be made continuously from islands in the equatorial Pacific.

6. Mixed layer depth should be resolved at all sites measuring air-sea fluxes and at other locations as well.

7. A subset of the flux stations should include observations of state variables and their covariance fluxes. Hopefully by 2020, the power requirements will be reduced sufficiently that these sensors could have a 1+ year endurance. These covariance flux sensors would additionally be able to monitor wave characteristics, and their influence on wind stress and fluxes. These sites could also carry Chi-pod sensors to monitor heat fluxes and mixing within the water column.

8. PAR and subsurface optical absorption should also be measured at one or more biogeochemical flux stations in a region of light wind where there may be feedbacks between the diurnal warm layer and phytoplankton blooms. Pending technology development, observations of the direct and diffuse radiation components at this station would provide invaluable information for the extinction

profile in water, for ocean heat budgets, and cloud studies. Efforts should be made to have the TPOS radiation measurements meet the standards of the Baseline Surface Radiation (BSRN) protocols (Ohmura et al. 1998).

9. Although barometric pressure has little effect on the flux estimate, it can be an important surface observation to assimilate and to observe for understanding the physics of the boundary layer system. Because atmospheric tides cause large variability in barometric pressure, isolated sensors can be difficult to interpret. But these are filtered out when considering BP gradients (e.g. 2N minus equator). A single BP in the tropics will be difficult to interpret, but pairs may be quite interesting.

Appendix 1 – TPOS array of 2005

The present and past TPOS buoy array can be viewed through the TAO data display and delivery webpage: http://www.pmel.noaa.gov/tao/data_deliv/deliv.html.

By selecting "Availability" on this webpage, one can see the full time and space coverage of the selected variables. Figure A1 shows the 2005 configuration of TPOS for each flux parameter. Figure A1 summarizes the flux capabilities of the global buoy array.
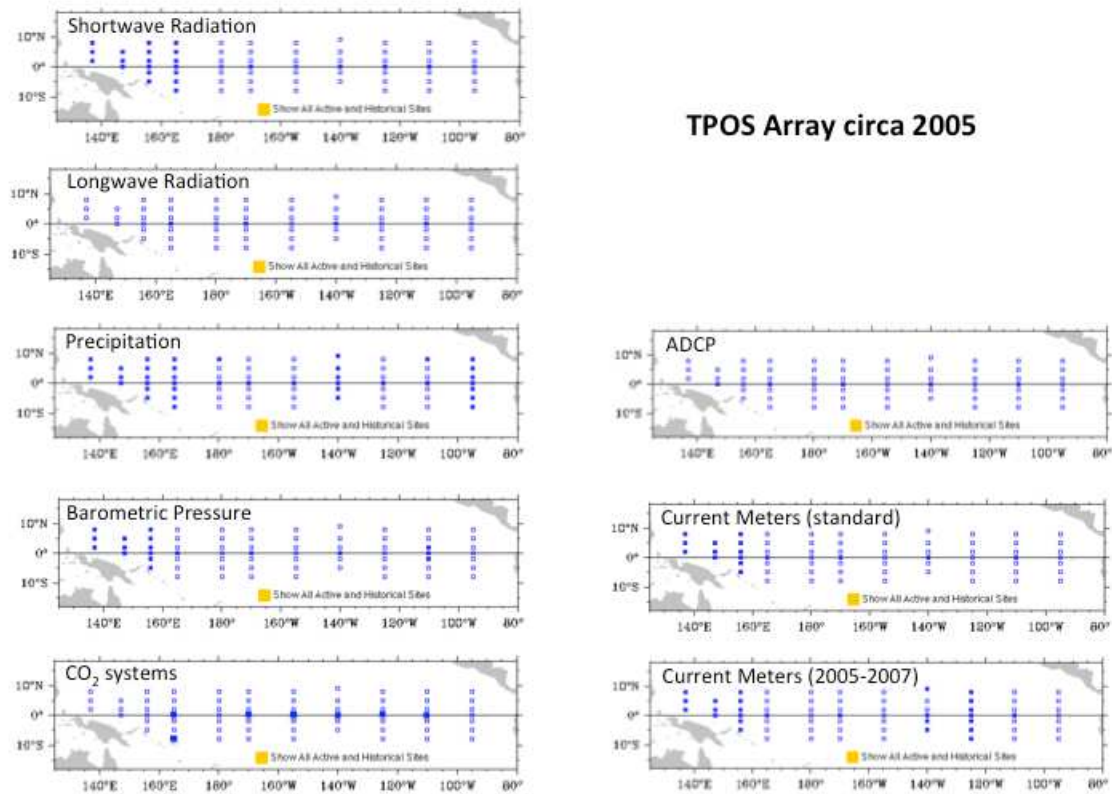

Figure A1 - Configuration of the 2005 TPOS for flux and flux parameters.

References

Anctil, F., Donelan, M.A., Drennan, W.M., and Graber, H.C. (1994): Eddy-Correlation Measurements of Air-Sea Fluxes from a Discus Buoy. J. Atmos. Oceanic Technol., 11, pp. 1144–1150.

Allan, R. P., Ringer, M.A., Pamment, J.A., and Slingo, A. (2004): Simulation of the Earth's radiation budget by the European Centre for Medium Range Weather Forecasts 40-year Reanalysis (ERA40) J. Geophys. Res., 109, D18107, (doi: 10.1029/2004JD004816).

Ashok, K., Behera, S.K., Rao, S.A., Weng, H., and Yamagata, T. (2007): El Niño Modoki and its possible teleconnection, J. Geophys. Res., 112, C11007, (doi: 10.1029/2006JC003798).

Balsley, B. B., Frehlich, R. G., Jensen, M. L., and Meillier, Y., (2006): High-Resolution In Situ Profiling through the Stable Boundary Layer: Examination of the SBL Top in Terms of Minimum Shear, Maximum Stratification, and Turbulence Decrease. J. Atmos. Sci., 63, pp. 1291–1307, (doi: 10.1175/JAS3671.1).

Betts, A. K., Zhao, M., Dirmeyer, P.A., and Beljaars, A.C.M. (2006): Comparison of ERA40 and NCEP/DOE near-surface data sets with other ISLSCP-II data sets, J. Geophys. Res., 111, D22S04, (doi:10.1029/2006JD007174).

Bigorre, S, Weller, R.A., Lord, J., Edson, J.B., and Ware, J.D. (2013): A surface mooring for air-sea interaction research in the Gulf Stream. Part 2: Analysis of the observations and their accuracies, J. Atmos. Oceanic Tech., 30, pp. 450–469.

Bosilovich, M. G., Chen, J., Robertson, F.R., and Adler, R.F. (2008): Evaluation of Global Precipitation in Reanalyses. J. Appl. Meteor. Climatol., 47, pp. 2279–2299. (doi: 10.1175/2008JAMC1921.1).

Bourassa, M. A. (2006): Satellite-based observations of surface turbulent stress during severe weather, Atmosphere - Ocean Interactions, Vol. 2., ed., W. Perrie, Southampton, UK, Wessex Institute of Technology Press, pp. 35 – 52.

Cai, W., and co-authors (2014): Increasing frequency of extreme El Niño events due to greenhouse warming. Nature Clim. Change, 4, pp. 111-116, (doi: 10.1038/nclimate2100).

Cardone, V.J. (1969): Specification of the wind distribution in the marine boundary layer for wave forecasting. Geophys. Sci. Lab. N.Y. Univ. Report TR-69-1 (NTIS AD 702-490).

Cardone, V.J., Jensen, R.E., Resio, D.T., Swail V.R., and Cox, A.T. (1996): Evaluation of contemporary ocean wave models in rare extreme events: the "Halloween Storm" of October, 1991 and the "Storm of the Century" of March 1993. Journal of Atmospheric and Oceanic Technology, 13, pp. 198–230.

Chelton, Dudley B., and Coauthors (2001): Observations of Coupling between Surface Wind Stress and Sea Surface Temperature in the Eastern Tropical Pacific. J. Climate, 14, pp. 1479–1498. (doi: 10.1175/1520-0442(2001)014<1479:OOCBSW>2.0.CO;2).

Chen, J., Del Genio, A.D., Carlson, B.E., and Bosilovich, M.G. (2008): The spatiotemporal structure of 20th-century climate variations in observations and reanalyses. Part I: Long-term trend. J. Climate, 21, pp. 2611–2633.

Clayson, C. A., and Bogdanoff, A.S. (2013): The Effect of Diurnal Sea Surface Temperature Warming on Climatological Air–Sea Fluxes. J. Climate, 26, pp. 2546–2556. (doi: 10.1175/JCLI-D-12-00062.1).

Clayson, C. A., Roberts, J.B., and Bogdanoff, A. (2014): SeaFlux Version 1: A new satellite-based ocean-atmosphere turbulent flux dataset. Int. J. Climatol., in revision.

Colbo, K., and Weller, R.A. (2009): Accuracy of the IMET Sensor Package in the Subtropics. J. Atmos. Oceanic Technol., 26, pp.1867–1890. (doi: http://dx.doi.org/10.1175/2009JTECHO667.1).

Collins, C., C. Reason, J.C., and Hermes, J.C. (2012): Scatterometer and reanalysis wind products over the western tropical Indian Ocean, J. Geophys. Res., 117, C03045, (doi:10.1029/2011JC007531).

Cronin, M. F., Bond, N. A., Fairall, C. W., and Weller, R. A. (2006a): Surface Cloud Forcing in the East Pacific Stratus Deck/Cold Tongue/ITCZ Complex. J. Climate, 19(3), pp. 392-409.

Cronin, M. F., Fairall, C.W., and McPhaden, M.J. (2006b): An assessment of buoy-derived and numerical weather prediction surface heat fluxes in the tropical Pacific, J. Geophys. Res., 111, C06038, (doi:10.1029/2005JC00332).

Cronin, M. F., Xie, S.P., and Hashizume, H. (2003): Barometric pressure variations associated with eastern Pacific tropical instability waves. J. Climate, 16, pp. 3050-3057.

Danabasoglu, G., Large, W.G., Tribbia, J.J., Gent, P.R., Briegleb, B.P., and McWilliams, J.C., (2006): Diurnal Coupling in the Tropical Oceans of CCSM3. J. Climate, 19, pp. 2347–2365. (doi: 10.1175/JCLI3739.1).

Deser, C., and Smith, C.A: (1998): Diurnal and semidiurnal variations of the surface wind field over the tropical Pacific Ocean, J. Clim., 11, pp. 1730–1748.

Donelan, M.A., Drennan, W.M., and Katsaros, K.B. (1997): The air-sea momentum flux in conditions of wind sea and swell. J. Phys. Oceanogr., 27, pp. 2087   2099.

Donlon, C.J., and Coauthors (2010): Successes and challenges for the modern sea surface temperature observing system: The Group for High Resolution Sea Surface Temperature (GHRSST) Development and Implementation Plan (GDIP), Community whitepaper for OceanObs09, Venice, Italy, 21-25 September, 2009.

Donlon, C.J., and Coauthors (2009): Successes and challenges for the modern sea surface temperature observing system: The Group for High Resolution Sea Surface Temperature (GHRSST) Development and Implementation Plan (GDIP), available from: https://www.ghrsst.org/files/download.php?m=documents&f=OO-ModernEraSST-v3.0.pdf.

Draper, D. W., and Long, D.G. (2004): Evaluating the effect of rain on scatterometer measurements. J. Geophys. Res., 109, (doi:10.1029/2002JC001741).

Edson, James B., and Coauthors (2013): On the Exchange of Momentum over the Open Ocean. J. Phys. Oceanogr., 43, pp. 1589–1610. (doi: 10.1175/JPO-D-12-0173.1).

Edson, J.B., Hinton, A.A., Prada, K.E., Hare, J.E., and Fairall, C.W. (1998): Direct covariance flux estimates from mobile platforms at sea, J. Atmos. Oceanic Tech., 15, pp. 547-562.

Fairall, C. W., Bradley, E.F., Hare, J.E., Grachev, A.A., Edson, J.B. (2003): Bulk Parameterization of Air–Sea Fluxes: Updates and Verification for the COARE Algorithm. J. Climate, 16, pp. 571–591. (doi: 10.1175/1520-0442(2003)016<0571:BPOASF>2.0.CO;2).

Fairall, C. W., Bradley, E.F., Rogers, D.P., Edson, J.B., and Young, G.S. (1996a): Bulk parameterization of air-sea fluxes for Tropical Ocean-Global Atmosphere Coupled-Ocean Atmosphere Response Experiment, J. Geophys. Res., 101, pp. 3747–3764, (doi:10.1029/95JC03205).

Fairall, C. W., Bradley, E.F., Godfrey, J.S., Wick, G.A., Edson, J.B., and Young, G.S. (1996b): Cool-skin and warm-layer effects on sea surface temperature, J. Geophys. Res., 101(C1), pp. 1295–1308, (doi:10.1029/95JC03190).

Fairall, C. W., Yang, M., Bariteau, L., Edson, J.B., Helmig, D., McGillis, W., Pezoa, S., Hare, J.E., Huebert, B., and Blomquist, B. (2011): Implementation of the Coupled Ocean-Atmosphere Response Experiment flux algorithm with CO_2, dimethyl sulfide, and O_3, J. Geophys. Res., 116, C00F09, (doi:10.1029/2010JC006884).

Freitag, H. P., Y. Feng, Y., Mangum, L.J., McPhaden, M.J., Neander, J., and Stratton, L.D. (1994): Calibration procedures and instrumental accuracy estimates of TAO temperature, relative humidity and radiation measurements. Tech. Memo. ERL PMEL-104 (PB95–174827), NOAA, Pacific Marine Environmental Laboratory, Seattle, WA, 32 pp.

Fung, I. Y., Harrison, D.E., and Lacis, A.A. (1984): On the variability of the net longwave radiation at the ocean surface, Rev. Geophys., 22, pp. 177–193.

Gill, Q. E. (1980): Some simple solutions for heat induced tropical circulations. Quart. J. Roy. Meteor. Soc., 106, pp. 447-462.

Gray, W. M., and Jacobson, R.W. (1977): Diurnal variation of deep cumulus convection, Mon. Weather Rev., 105, pp. 1171–1188.

Griffies, S.M., Biastoch, A., Boening, C., and Belyaev, K. (2012): Probability distribution characteristics for air-sea turbulent heat fluxes over the global ocean. J. Climate, 25, pp. 184-206.

Gupta, S. K., Darnell, W.L., and Wilber, A.C. (1992): A parameterization for longwave surface radiation from satellite data: Recent improvements, J. Appl. Meteorol., 31, pp. 1361–1367, (doi:10.1175/1520-0450).

Holbach, H. M., and Bourassa, M.A. (2013): The effects of gap–wind–induced vorticity, the monsoon trough, and the ITCZ on tropical cyclogenesis. Mon. Wea. Rev. (in press).

Jackson, D. L., and Wick, G.A. (2010): Near-Surface Air Temperature Retrieval Derived from AMSU-A and Sea Surface Temperature Observations. J. Atmos. Oceanic Technol., 27, pp. 1769–1776.

Jin, X., and Yu, L. (2013): Assessing high-resolution analysis of surface heat fluxes in the Gulf Stream region. J. Geophys. Res., 118, (doi: 10.1002/jgrc.20386).

Kara, A. B., Wallcraft, A.J., and Bourassa, M.A. (2008): Air-Sea Stability Effects on the 10m Winds Over the Global Ocean: Evaluations of Air-Sea Flux Algorithms. J. Geophys. Res., 113, C04009, (doi:10.1029/2007JC004324).

Large, W. G., and Yeager, S.G. (2009): The global climatology of an interannually varying air-sea flux data set. Climate Dynamics, 33, pp. 341-364 (doi: 10.1007/s00382-008-0441-3).

Lengaigne, M., and Vecchi, G.A. (2010): Contrasting the termination of moderate and extreme El Niño events in Coupled General Circulation Models. Climate Dynamics, (doi: 10.1007/s00382-009-0562-3).

Lloyd, J., Guilyardi, E., Weller, H., and Slingo, J. (2009): The role of atmosphere feedbacks during ENSO in the CMIP3 models. Atmos. Sci. Lett. 10 (3), pp. 170-176.

Marshall, J., Andersson, A., Bates, N., Dewar, W., Doney, S., Edson, J., Ferrari, R., Forget, G., Fratantoni, D., Gregg, M., Joyce, T., Kelly, K., Lozier, S., Lumpkin, R., Maze, G., Palter, J., Samelson, R., Silverthorne, K., Skyllingstad, E., Straneo, F., Talley, L., Thomas, L., Toole, J., and

Weller, R. (2012): "The CLIMODE field campaign: Observing the cycle of convection and restratification over the Gulf Stream," Bull. Amer. Meteor. Soc., 90, pp. 1337-1350.

May, J., and Bourassa, M.A. (2011): Quantifying variance due to temporal and spatial difference between ship and satellite winds. J. Geophys. Res., 116, (doi:10.1029/2010JC006931).

McGillis, W. R., Edson, J.B., Hare, J.E., and Fairall, C.W. (2001): Direct covariance air-sea CO_2 fluxes, J. Geophys. Res., 106, pp. 16729-16745.

McPhaden, M. J., Busalacchi, A. J., Cheney, R., Donguy, J.-R., Gage, K. S., Halpern, D., Ji, M., Julian, P., Meyers, G., Mitchum, G. T., Niiler,P. P., Picaut, J., Reynolds, R. W., Smith, N., and Takeuchi, K. (1998): The Tropical Ocean-Global Atmosphere observing system: A decade of progress. J. Geophys. Res. 103, C7, pp. 14169–14240, (doi:10.1029/97JC02906).

Milliff, R. F., Morzel, J., Chelton, D.B., and Freilich, M.H. (2004): Wind stress curl and wind stress divergence biases from rain effects on QSCAT surface wind retrievals, J. Atmos. Oceanic Technol., 21, pp. 1216–1231.

Moum, J. N., Perlin, A., Nash, J.D., and McPhaden, M.J. (2013): Ocean mixing controls seasonal sea surface cooling in the equatorial Pacific cold tongue. Nature, 500, pp. 64-67.

Murtugudde, Raghu, Beauchamp, J., McClain, C.R., Lewis, M., Busalacchi, A.J. (2002): Effects of Penetrative Radiation on the Upper Tropical Ocean Circulation. J. Climate, 15, pp. 470–486. (doi: 10.1175/1520-0442(2002)015<0470:EOPROT>2.0.CO;2).

Newman, M., Sardeshmukh, P.D., and Bergman, J.W. (2000): An Assessment of the NCEP, NASA, and ECMWF Reanalyses over the Tropical West Pacific Warm Pool. Bull. Amer. Meteor. Soc., 81, pp. 41–48. (doi: 10.1175/1520-0477(2000)081<0041:AAOTNN>2.3.CO;2).

Ohmura, A., DeLuisi, J., Dutton, E., Heimo, A., Forgan, B., Pinker, R.T., Frohlich, C., Philipona, R., Konig-Langlo, G., Whitlock, C., McArthur, B., and Dehne, K. (1998): Baseline Surface Radiation Network (BSRN/WCRP), a new precision radiometry for climate research. Bull. Am. Met. Soc., 79, No. 10, pp. 2115-2137.

Patara, L., Vichi, M., Masina, S., Fogli, P.G., and Manzini, E. (2012): Global response to solar radiation absorbed by phytoplankton in a coupled climate model. Clim. Dyn., 39, pp. 1951-1968.

Pinker, R. T., Bentamy, A., Katsaros, K.B., Ma, Y., and Li, C. (2013): Estimates of net heat fluxes over the Atlantic Ocean. JGR-Oceans. Accepted, JGR-Oceans.

Prytherch, J., Kent, E.C., Fangohr, S., and Berry, D.I. (2013): A comparison of satellite-derived global marine surface specific humidity datasets. Int. J. Climatol., in revision.

Randall, D., Harshvardhan, A., and Dazlich, D.A. (1991): Diurnal variability of the hydrological cycle in a general circulation model, J. Atmos. Sci., 48, pp. 40–62.

Roberts, J. B., Clayson, C.A., Robertson, F.R., and Jackson, D. (2010): Predicting near-surface characteristics from SSM/I using neural networks with a first guess approach. J. Geophys. Res., 115, D19113, (doi: 10.1029/200d9JD013099).

Ross, D.B., Cardone, V.J., Overland, J., McPherson, M., Pierson, R.D., and Yu, T. (1985): Oceanic surface winds. Adv. Geophys., 27, pp. 101–138.

Seo, K.H., Wang, W., Gottschalck, J., Zhang, Q., Schemm, J.K.E., Higgins, W.R., and Kumar, A. (2009): Evaluation of MJO Forecast Skill from Several Statistical and Dynamical Forecast Models. J. Climate, 22, pp. 2372–2388.

Serra, Y.L., A'Hearn, P., Freitag, H.P., and McPhaden, M.J. (2001): ATLAS self-siphoning rain gauge error estimates. J. Atmos. Ocean. Technol., 18, pp. 1989-2002.

Siegel, D. A., Ohlmann, J.C., Washburn, L., Bidigare, R.R., Nosse, C.T., Fields, E., and Zhou, Y. (1995): Solar radiation, phytoplankton pigments and the radiant heating of the equatorial Pacific warm pool. J. Geophys. Res., 100(C3), pp. 4885–4891, (doi:10.1029/94JC03128).

Song, X., and Yu, L. (2013): How much net surface heat flux should go into the Western Pacific Warm Pool? J. Geophys. Res., 118, pp. 3569-3585, (doi: 10.1002/jgrc.20246).

Smith, S., Hughes, P., and Bourassa, M. (2011): A comparison of nine monthly air-sea flux products. Internat. J. Climatol., 31, pp. 1002-1027, (doi: 10.1002/joc.2225).

Stiles, B. W., Danielson, R.E., Poulsen, W.L., Brennan, M.J., Hristova-Veleva, S., Shen, T.P.J., and Fore, A.G. (2013): Optimized Tropical Cyclone Winds from QuikSCAT: A Neural Network Approach. TGARS, in press.

Takahashi, K., Montecinos, A., Goubanova, K., and Dewitte, B. (2011): ENSO regimes: Reinterpreting the canonical and Modoki El Niño, Geophys. Res. Lett., 38, L10704, (doi:10.1029/2011GL047364).

Takahashi, K. (2012): Thermotidal and land-heating forcing of the diurnal cycle of oceanic surface winds in the eastern tropical Pacific. Geophys. Res. Lett. 39, L04805, (doi:10.1029/2011GL050692).

Trenberth, K. E., Branstator, G.W., Karoly, D., Kumar, A., Lau, N.C., and Ropelewski, C. (1998): Progress during TOGA in understanding and modeling global teleconnections associated with tropical sea surface temperatures. J. Geophys. Res., 103 (special TOGA issue), pp. 14291-14324.

Ueyama, R., and Deser, C. (2008): A climatology of diurnal and semidiurnal surface wind variations over the tropical Pacific Ocean based on the tropical atmosphere ocean moored buoy array, J. Clim., 21, pp. 593–607.

Wallace, J.M., and Gutzler, D.S. (1981): Teleconnections in the Geopotential Height Field during the Northern Hemisphere Winter. Mon. Wea. Rev., 109, pp. 784–812.

Wang, J., Rossow, W.B., and Zhang, Y. (2000): Cloud vertical structure and its variations from a 20-yr global rawinsonde dataset. J. Climate, 13, pp. 3041–3056, (doi:10.1175/1520-0442).

Ware, R., Carpenter, R., Güldner, J., Liljegren, J., Nehrkorn, T., Solheim, F., and Vandenberghe, F. (2003): A multichannel radiometric profiler of temperature, humidity, and cloud liquid, Radio Science, (doi:10.1029/2002RS002856).

Weissman, D. E., Stiles, B.W., Hristova-Veleva, S.M., Long, D.G., Smith, D.K., Hilburn, K.A., and Jones, W.L. (2012): Challenges to satellite sensors of ocean winds: Addressing precipitation effects. J. Atmos. Oceanic Tech., 29, pp. 356-374

Weissman, D. E., Bourassa, M.A., and Tongue, J. (2002): Effects of rain rate and wind magnitude on SeaWinds scatterometer wind speed errors. J. Atmos. Ocean. Tech., 19, pp. 738-746.

Weller R. A., Bigorre, S. P., Lord, J., Ware, J.D., and Edson, J.B. (2012): A surface mooring for air-sea interaction research in the Gulf Stream. Part 1: Mooring design and instrumentation, J. Atmos. Ocean. Tech., 29, pp. 1363-1376.

Yu, L., Jin, X., and Weller, R. (2008): Multidecade global flux datasets from the Objectively Analyzed Air-sea Fluxes (OAFlux) project: Latent and sensible heat fluxes, ocean evaporation, and related surface meteorological variables. OAFlux Project Tech. Rep. OA-2008-01, 64 pp.

Zhang, C., McGauley, M., and Bond, N.A. (2004): Shallow Meridional Circulation in the Tropical Eastern Pacific. J. Climate, 17, pp. 133–139.